Relationship of Inflammation/Thrombosis and C-reactive protein (CRP), Plasminogen Activator Inhibitor 1 (PAI-1), Inteleukin-6 (IL-6), Inteleukin-1 (IL-1), Tissue Factor (TF), Tumor Necrosis Factor-alpha (TNF-α), tTssue Plasminogen Activator (tPA), CD40

Ma Hongbao *, Cherng Shen **

* Michigan State University, East Lansing, MI 48824, USA
mahongbao2000@yahoo.com

** Department of Electrical Engineering, Chengshiu University, Niaosong, Taiwan 833, Republic of China, cherngs@csu.edu.tw, 011886-7731-0606 ext 3423

Abstract: This project is to elucidate the relationship between systemic inflammation and plaque disruption and thrombosis. The implications of this could greatly define the mechanism leading to acute cardiovascular events including myocardial infarction and strokes. Also, this could lead to novel therapeutic and preventive approaches. The proposal seeks to investigate the kinetics of inflammation markers prior to and during an acute cardiovascular event. The feasibility depends on a valuable model developed by Dr. Abela's laboratory. This is an atherosclerotic rabbit model that can be pharmacologically triggered to develop plaque disruption and thrombosis. Thus, the inflammatory process can be monitored through an event. This rabbit atherosclerotic model is ideally suited to test potential therapeutics. **Specific Aim 1** will investigate the mechanism of C-reactive protein (CRP) in the development of acute thrombosis. CRP has been shown to increase plasminogen activator inhibitor 1 (PAI-1) and tissue factor (TF) in cell culture. This will be evaluated in an *in vivo* model and the kinetics and sequence of expression of markers will be demonstrated in the applied project. CRP effects on TF and CD-40L/CD-40 pathway activation will be evaluated. Platelet aggregation and adhesion will be measured in atherosclerotic rabbits with higher soluble CD40L following vascular injury in a dual organ perfusion chamber with and without antiplatelet agents. CRP, TF, IL-6 and CD40 will be evaluated following thrombus triggering in 20 rabbits compared to 20 control rabbits. **Specific Aim 2** will use immunohistochemical methods to demonstrate the localization of inflammatory markers in the arterial wall with local temperature rise. **Specific Aim 3** will use thermal model to analyze the generation of local temperature following vascular injury. This will be done both in a special *in vitro* thermally isolated and *in vivo*. **Specific Aim 4** will study the relationship between the inflammation factors and the effect of UV excimer laser on the thrombosis in the atherosclerotic rabbit. [Nature and Science. 2007;5(4):61-74].

1. Specific Aims

In order to study relationship of inflammation and thrombosis, an atherosclerotic rabbit model will be used (1) and C-reactive protein (CRP), plasminogen activator inhibitor 1 (PAI-1), inteleukin-6 (IL-6), inteleukin-1 (IL-1), tissue factor (TF), tumor necrosis factor-alpha (TNF-α), tissue plasminogen activator (tPA), CD40, and temperature will be measured.

Specific Aim 1. To Determine the Mechanism of CRP-mediated Vascular Thrombosis.

Aim 1a will test the hypothesis that increased serum CRP induces thrombosis by increasing PAI-1 and TF levels. We propose to determine *in vivo* physiological mechanisms underlying CRP induced PAI-1 and TF by investigating the kinetics of CRP, PAI-1 and TF level changes.

Aim 1b will test the hypothesis that CRP induced TF is mediated via CD40/CD40L (CD40 ligation) activated pathway, and CRP mediated upregulation of PAI-1 is mediated by inhibition of tPA leading to acute thrombus formation *in vivo*. Time-course immunohistochemical studies will be conducted to determine the localization of CD40, CD40L, TF, tPA and PAI-1.

Aim 1c. To test the specificity of CRP, PAI-1, and TF mediated thrombosis, we will administer neutralizing antibodies to CRP, PAI-1, and TF to reduce the thrombotic events.

Aim 1d will test the hypothesis that platelets from rabbits with atherosclerosis will have significantly higher levels of soluble CD40/CD40L production.

Specific Aim 2. Mechanism of Injury-induced Arterial Wall Temperature Increase and Mediatory Role of CRP.

Aim 2a. Using temperature measurement as a diagnostic marker of intensity of the inflammatory response, the arterial wall temperature will be measured at sites of arterial injury and correlated to the changes in serum CRP concentrations.

Aim 2b will evaluate the relationship among tissue cholesterol levels, expression levels of CRP, PAI-1, tPA, TF, CD40/CD40L, and local temperature rise in the aortic atherosclerotic plaques. To determine the causative factors of temperature rise in the atherosclerotic lesions, we propose to determine levels of CRP, PAI-1, tPA, TF and CD40/CD40L in the atherosclerotic plaques and correlate these data to arterial wall temperature and cholesterol levels.

Aim 2c will evaluate the effect of administration of antibodies directed against TF, CD40, CD40L, PAI-1 and tPA and CRP antibodies on the changes in arterial wall temperatures.

Specific Aim 3. Thermal Modeling of Injury Site to Obtaining Quantitative Relationships Between the Rate of Heat Generation and Associated Temperature Rise.

Aim 3a will determine the heat released during clotting of blood using a calorimeter experiment. The information can in turn be utilized to calculate the expected temperature rise associated with clotting in an artery in the body.

Aim 3b. Using numerical methods for the heat transfer processes involved in the arteries, estimates can be prepared relating the amount of heat generated to the temperature rise expected in response to the heat addition.

Aim 3c. Using methods of inverse heat transfer analysis, measurements taken in Specific Aim 2 can be analyzed to compute the amount of heat generated at the site of an injury.

Specific Aim 4: Relationship Between Inflammation Factors and Effect of Excimer Laser Ablation of Thrombus.

Aim 4a will test the effect of UV excimer laser on thrombosis in atherosclerotic rabbit. Our previous *in vitro* studies showed that UV excimer laser alters platelet aggregation based on total energy and greater laser power resulted in higher rate of thrombus ablation (2).

Aim 4b will study if the inflammation factors in the serum of rabbit are correlated to the UV excimer laser effect on thrombus formation/ablation and platelet activities *in vitro* and *in vivo*.

2. Background and Significance

2.1 Atherosclerosis, Systemic Inflammation and Thrombosis.

Increasing number of studies has demonstrated that atherosclerosis is associated with inflammation and acute coronary events. Buffon et al demonstrated that in an acute cardiovascular event related to a lesion in one coronary artery was associated with inflammation in the adjacent and non-involved artery by angiography (3). A compelling amount of data using different technologies have demonstrated that often more than one plaque is ruptured both in the culprit artery with thrombosis and in adjacent non-occluded arteries at the time of an acute myocardial event (4). Rioufol et al demonstrated multiple atherosclerotic plaque ruptures in patients during acute coronary syndrome by conducting intravascular ultrasound scan of all three coronary arteries in 24 patients with acute coronary syndrome (5). Furthermore, patients with acute cardiovascular events seem to have plaques that have ruptured in other arterial beds such as the carotid arteries at the time of the event (6). Thus, it is almost inevitable to assume that the outcome at a specific arterial site is being influenced by a systemic process. Additional supportive data regarding the systemic nature and effects of atherosclerosis comes from the strong association between peripheral vascular disease and coronary artery disease (7). In fact, carotid arterial wall thickness has been used as a strong index of coronary artery disease and predictor of future events (8). Also, as with coronary artery disease, the elevation in CRP is an indicator of future development of claudication and symptomatic peripheral vascular disease (9). All these observations seem to support that coronary artery disease is part of a systemic condition reflected by the presence generalized inflammation. Further, as with coronary artery disease, the elevation in CRP is an indicator of future development of claudication and symptomatic peripheral vascular disease. Systemic inflammatory marker CRP also has recently been shown to play an important role in promotion of atherothrombosis by increasing recruitment of monocytes (10) and by increasing recruited monocyte synthesis of TF (11). It has also been shown that CRP exerts its proatherothrombotic effect directly on endothelial cells (ECs) by increasing PAI-1 in the EC resulting in platelet aggregation and thrombosis. PAI-1, a marker of impaired fibrinolysis exert its atherothrombogenic effects by inhibiting

conversion of inactive plasminogen to active plasmin, a fibrin-degrading protease, by binding and inactivating tPA and urokinase plasminogen activator (12, 13). Further, PAI-1 has been shown to have the highest affinity for tPA in plasma and thus has been suggested to be the major regulator of tPA activity in the blood (14). Indeed, decreased fibrinolysis due to increased PAI-1 activity, PAI-1 and tPA complexes, and decreased tPA levels have been demonstrated in patients with coronary artery disease. PAI-1 is also increased in atherosclerotic plaques, and blood of patients with atherosclerosis, especially increased in diabetic patients (15). Interestingly, diabetic patients are known to be at greater risk for acute cardiovascular events. Also, CRP is markedly higher in patients with metabolic syndrome as well as diabetes (16). Importantly, increased PAI-1 levels have been shown to enhance thrombosis, and administration of antibodies directed against PAI-1 has been shown to be effective in prevention of the thrombosis development (17-21). Furthermore, a recent study has shown that transgenic mice expressing human PAI-1 develop coronary arterial thrombosis (22). CD40 a membrane-bound glycoprotein is expressed in B lymphocytes, dendritic cells, monocytes, and ECs (23). Its ligand, CD40L is expressed in activated T cells, smooth muscle cells, macrophages (23, 24) and activated platelets (25). Further, procoagulant activity of platelets has been shown to be via the CD40/CD40L pathway (25, 26). Importantly, recent study has shown that activated platelets increase TF in human monocytes (27). Since TF expression in monocytes and macrophage has been shown to be induced by cross-linking processes, it is plausible that CD40L expressing platelet interaction with CD40 expressing monocytes and macrophages cross link to induce TF production from the monocytes and macrophages. Interestingly, an increasing number of studies support a key role for the CD40/CD40L pathway in atheroma progression. Patients with unstable angina have significantly higher levels of soluble and membrane-bound forms of CD40L (28). Recent studies have also suggested that activated platelets can express CD40L and trigger inflammatory response and TF expression in ECs through interaction with CD40 (29). The linkage between systemic inflammation and coagulation, and possibly thrombosis may involve TF. Circulating TF is detected in patients with unstable angina (30), and high levels are expressed on macrophages in unstable plaques (31). It has also been shown in monocytes that CRP induces the production of inflammatory cytokines and promotes monocyte chemotaxis and TF expression (10, 11). Increased monocyte TF expression during infection or tissue necrosis may be at least partially mediated by an increased CRP level (11). This study and others strengthen the hypothesis that CRP is associated with clinical events by altering clotting status through induction of monocyte TF (11, 32).

2.2 Arterial Wall Temperature as a Reflection of Inflammation.

A strong physical marker for inflammation is temperature elevation. In fact, inflammation has been traditionally defined by ‘calor’ - heat , ‘rubor’ - redness, ‘dolor’ - pain and ‘turgor’ - swelling. Recently, studies have demonstrated that increased arterial temperature as an index of inflammation may be a marker of increased risk for plaque rupture and thrombosis. Cassells et al demonstrated temperature elevation at specific sites of plaques extracted during carotid endarterectomy procedures. At histologic examination, the sites with higher temperature had a greater concentration of inflammatory cell density (33). Stephanadies et al conducted several studies measuring temperature in human coronary arteries using a thermal sensing catheter. They demonstrated a wide local temperature dispersion in coronary arteries of patients who presented with acute cardiovascular events but not in patients with normal arteries or stable angina symptoms (34). Both the physical and the biochemical data seem to track together suggesting that both temperature and elevation in inflammatory molecules are involved in the process leading to and possibly causing the acute cardiovascular event. However, it is probably thrombus formation that is the common end pathway that is the result of this process. Thus, thrombus formation may be a common denominator that can be used to access the extent of local inflammation.

Despite some inconsistencies in the temperature measurements in detecting “vulnerable plaque”, detection of local inflammation and thrombus may be equally valuable data in the assessment of immediate outcome and potential future cardiovascular events. Thermistors have been used with sinusoidal heating to determine thermal parameters in small arteries. This work by Anderson and Valvano (35) was performed in canine kidneys, but has wide applicability for arterial thermal measurements. Studies of heat transfer in blood flow in artery and vein pairs have been studied by Roemer (36). Analytical solutions were compared to numerical calculations for heat transfer in blood vessels by Zhu and Weinbaum (37). Green's functions were used in the exact solutions in this work and axial variation was observed with this formulation for the first time. Radiative heating of biological tissues was examined by Klemick et al (38). A numerical grid

was used in this work, which would be similar to the analysis proposed presently. A solution of the Pennes equation was given by Chan (39) using the boundary element method. As a predecessor to the work by Zhu and Weinbaum (37), this solution did not allow temperature variation in the axial direction. The body of research for arterial heat transfer is mature enough to allow a solid foundation on which to compute temperature rises due to the biochemical reactions, proposed for investigation as part of the present proposal.

3. Preliminary Studies

3.1 Cholesterol Content Was Directly Correlated With Amount of Thrombosis. Using the atherosclerotic rabbit model of plaque disruption and thrombosis, we demonstrated that the amount of cholesterol content in arterial wall is directly correlated with amount of thrombus formation (r=0.98; p=0.003) (40).

3.2 CRP Increased Significantly with Thrombus Formation. With the atherosclerotic rabbit model our results showed that levels of CRP increased significantly with thrombus formation (41). Also, pravastatin preserves vasomotor response after balloon angioplasty (42) and beta-carotene preserves endothelium dependent relaxation in atherosclerotic rabbits (43).

3.2 Possible Mechanism of Systemic Inflammation Mediated Local Thrombosis. **With the same model as 3.1, results showed that rabbit serum IL-6 concentration increase and reached peak level by 24 hours after thrombus triggering. This rise in IL-6 levels was preceded by the subsequent rise of serum CRP from 24 hours after Russell viper venom (RVV) and histamine administration reaching the peak levels by 48 hours. Sustained CRP as well IL-6 levels were observed from 48 to 72 hours. Interestingly, we observed concurrent rise of IL-6 and PAI-1 up to 24 hours. Importantly, the delayed second increases of serum PAI-1 levels were observed from 60 hours after RVV and histamine triggers. Immunohistochemical staining of section from thoracic aorta of atherosclerotic rabbits demonstrated that TF presented in the sites where thrombus formed.**

3.3 *In vitro* Testing of the Thermal Response of Arteries to Injury. With a dual perfusion chamber to measure the temperature of arteries injured by balloon catheter, our results showed that temperature rose of approximately $1^{o}C$ at the injured location.

3.4 *In vivo* Vascular Injury Elicits a Local Temperature Response. At 48 hours after rabbit thrombus triggering, a 4F special thermal catheter was advanced via a femoral cut down using fluoroscopic guidance. Temperature increased in the thrombus present site but not in the thrombus absent site.

3.5 Continuous Platelet Aggregation Measurement Using Laser Light Scattering. Using laser light scattering method to continuously measure platelet aggregation and ^{111}In-labeled platelets to measure platelet adhesion, we showed that platelet activity was increased when the platelet passed through an injured artery (44, 45).

3.6 Effect of Laser on Platelet Function and Stress Protein. Platelet rich plasma (PRP) circulating in a chamber was lased by 308 nm UV excimer laser with various energies and the platelet aggregation was measured by laser light scattering. The results showed that at the lower laser energy there was no significant platelet aggregation while at higher energies there was a significant increase in platelet aggregation (2). Heat shock protein 70 is reduced in rat myocardium following transmyocardial laser revascularization (46).

3.7 Effects of Aspirin on Platelets During Laser Procedure. Using the dual organ chamber, the results demonstrate a significant reduction in platelet aggregation by aspirin when measured by laser light scattering method.

3.8 Type and Amount of Debris Formed by Laser Ablation. Rabbit thrombi were formed by fibrinogen (5 mg/ml), thrombin (0.3 unit/ml) and $CaCl_2$ (1.5 mg/ml) then lased by UV excimer laser. The results demonstrated that at higher energies and catheter size resulted in greater amount of thrombus ablation and debris generation.

3.9 Gross and SEM of Thrombus Debris Formed by Laser Ablation. Gross and SEM images demonstrated that size, shape and structure of thrombus debris formed by excimer laser were correlated to the accumulated laser energy.

3.10 Hemoglobin Release into Medium. After lasing 1 ml rabbit whole blood with 2.0 mm fiber at 35 mJ/pulse and 10 Hz for 1 min, about 25% hemoglobin was released into the buffer.

4. Research Design and Methods

Rabbit Atherosclerosis Inducing and Thrombus Triggering (1): Each year, fifty NZW rabbits will be used. Control-control group (n=10) rabbits are fed a regular diet for 6 months. Control group (n=20) and thrombus group (n=20) rabbits are undergone balloon deendothelialization and were then maintained on a 1% cholesterol enriched diet (Harlan-Sprague Dawley, Inc., Indianapolis, IN) alternating with regular diet every month for a total of 6 months. Under general anesthesia (ketamine 50 mg/kg and xylazine 20 mg/kg, i.m.) balloon-induced deendothelialization of the aorta is performed using a 4F Fogarty arterial embolectomy catheter (Baxter Healthcare Corporation, Irvine, CA) introduced through the right femoral artery cutdown. The catheter was advanced in a retrograde fashion to the ascending aorta and pulled back three times. Thrombus group rabbits will be triggered thrombus by RVV (0.15 mg/kg, i.p., Sigma Chemical Co., St. Louis, MO) and histamine (0.02 mg/kg, i.v., Sigma Chemical Co., St. Louis, MO).

Aim 1a. Our preliminary data showed that serum CRP levels are significantly higher in the atherosclerotic rabbits, which have thrombi, compared to the atherosclerotic rabbits without thrombi formation *in vivo* (41). To determine whether two of the major regulators of thrombosis (PAI-1 and TF) are involved in CRP-associated thrombosis, venous blood will be collected from the ear vein at an interval of 6 to 72 hours from the cholesterol fed atherosclerotic rabbits post administration of RVV and histamine. The serum will be immediately stored at -80°C until further use. To measure kinetics of CRP-mediated thrombosis, time-dependent changes of serum CRP, PAI-1, IL-6, IL-1, TNF-α, and estrogens will also be investigated using ELISA. Briefly for rabbit CRP ELISA, 50 µl of anti-rabbit IgG capture antibody will be added to each well of 96-well plates (Dynatech Laboratories, Chantilly, VA) and incubated overnight at 4°C. The wells will be then washed with phosphate buffered saline (PBS) containing 0.1% tween 20, and 50 µl of rabbit serum diluted in 1:1000 ratio in 10% fetal bovine serum (FBS) and 1× PBS were added to each well. The wells will be washed and 10 µg of horseradish peroxydase conjugated anti-rabbit IgG detection antibodies will be added. The wells will be then washed with PBS containing 0.1% tween 20 prior to addition of 65 µl of 5,5 -tetramethyl- benzidine (TMB) liquid substrate. Within 30 minutes following addition of TMB substrate, the reaction will be stopped with 100 µl of 1 M H_2SO_4. The absorbance at 450 nm will be measured using microplate reader (Molecular Device, Sunnyvale, CA). IL-6, IL-1 and TNF-a levels will be measured using ELISA kits (BD Bioscience, San Jose, CA). Serum PAI-1 levels will be measured using rabbit PAI-1 kit according to the manufactures instructions (Molecular Innovations, Southfield, MI). To measure changes in TF pathway of blood coagulation, factor VII coagulant activity will be measured using plasma prepared at room temperature to avoid cold activation before being frozen at -80°C. FVII coagulant activity (FVIIc) will be then determined in a two-stage chromogenic assay containing thromboplastin (CoA-Set FVII, Chromogenics AB, Mølndal, Sweden).

Aim 1b will test the hypothesis that CRP induced TF is mediated via CD40/CD40L activated pathway, and CRP mediated upregulation of PAI-1 is mediated by inhibition of tPA leading to acute thrombus formation *in vivo*. To address this specific aim, time-course studies will be conducted to identify the portion of CD40, CD40L, TF, tPA and PAI-1 secreting cells using fixed peripheral blood from atherosclerotic rabbits. Briefly, peripheral blood will be fixed with addition of 1% formaldehyde followed by dilution at 1:200 with PBS. Erythrocytes will be removed by addition of FACS lysis solution for 10 minutes at room temperature. Samples will then be incubated for 30 minutes at room temperature with various antibodies including fluorescein isothiocyanate (FITC)–conjugated anti-CRP, anti-CD40, anti-CD40L, anti-TF and anti-PAI-1. Approximately 10^4 cells will be analyzed by FACS Vantage equipped with a G3 Mac computer and CellQuest software (Becton-Dickinson, San Jose, CA). Monocytes will be identified by gating for $CD14^+$ cells. T cells will be identified by gating for $CD4^+$ cells and $CD61^+$ will be used for identifying platelets. Furthermore, the levels of arterial wall cholesterol will be correlated to the serum levels of CRP and to the tissue levels of CD40, CD40L, TF, tPA, PAI-1.

For immunohistological analysis, rabbit aortas will be rapidly removed and frozen in liquid nitrogen followed by snap-freeze in OCT compound (Tissue-Tek) after the rabbit are killed. Cryostat sections (7 µm) of the aorta will be prepared, and air-dried 30 minutes at room temperature prior to washing with 0.1 M PBS followed staining with the respective antibody: anti-CD40, anti-CD40L, anti-TF and PAI-1, and anti-CRP. As negative controls, isotype control IgG will be used. After incubation with the appropriate biotinylated, affinity-purified secondary antibodies, the sections will be incubated with alkaline phosphatase-labeled streptavidin solution and visualized using a fast red substrate kit. Quantitative analysis of atherosclerotic lesions was performed by a single observer blinded to the experiment protocol. All images will be captured by microscope equipped with camera and analyzed using Adobe Photoshop 6.0 and

National Institute of Health Image 1.62 Software. For all samples, the average value for 5 locations for each animal will be used for analysis.

Aim 1c. To test the specificity of CRP, PAI-1 and TF mediated thrombosis, we will administer neutralizing antibodies to CRP, PAI-1 and TF to reduce the thrombotic events. Administration of CD40 and CD40L antibodies will also be conducted to demonstrate the specificity of CD40/CD40L mediated TF upregulation. Selected or acceptable antibodies will be injected intraperitoneally at doses 50, 100, 250, 500, and 1000 μg prior to administration of RVV and histamine for additional 72 hours. All animals will be killed at the end of 12, 24, 48 and 72 hours post RVV and histamine injection. Aortic thrombi formation will be examined as previously described. The number and size of thrombi will be measured using planimetry of digitized images of the aorta after exposure of the intimal surface. Also, total serum creatine kinase (CK) levels will be obtained. Serum will be obtained prior to triggering and at 12, 24, 48 and 72 hours post triggering. CK activity will be analyzed using U-V vis spectrophtometer (Hewlett-Packard 8542A U-V, Palo Alto, CA). This will provide an index of myocardial infarct size. Furthermore, triphenyltetrazolium chloride staining will be used to determine the amount of remaining viable myocardium and unstained infracted areas. Surface areas of infarction proportional to viable myocardium will be determined at four levels starting at the apex to the base of the heart.

Aim 1d will test the hypothesis that platelets from rabbits with atherosclerosis will have significantly higher levels of soluble CD40/CD40L production. Using a dual organ perfusion chamber, we will evaluate platelet aggregation and activation of platelets that have a greater production of soluble CD40L in the presence and absence of anti-inflammatory agents (such as aspirin, ibrufen, statin). Measurement of soluble CD40L will be analyzed by using commercially available ELISAs (Bender MedSystems, San Bruno, CA). Platelet aggregation and adhesion will be measured as previously reported by the PI using a unique method of laser light scattering (44). The advantages of this system are that it allows for continuous real time measurement of platelet aggregation over time. Furthermore, it allows simultaneous comparison of platelet aggregation after circulation through balloon injured arteries in the presence or absence of various antiplatelet agents. Also, it provides a means to evaluate platelet adhesion to the injured arteries by using ^{111}In-labeled platelets added to the circuit. The technique relies on the scattering of a He-Ne laser beam passed through cuvettes connected to tubing that drain the balloon-injured arteries. From the angle of incidence of the scattered light, the average volume of aggregates and the number of particles can be calculated from the ratio of the scattering light at 1 to 5 degrees spread on a diode array of a multichannel analyzer.

Aim 2a. We have previously demonstrated that temperature will rise at the site of acute vascular injury using balloon catheters. This is associated with the development of thrombus. In fact, temperature rise seems to be correlated with the development of thrombosis. Under general anesthesia, rabbits will be catheterized using fluoroscopic guidance. A right femoral cut down will be used to access a 4.5F introducer and 4F balloon catheter to induce arterial wall injury. Vertebrae will be used as landmarks to identify these sites for post-mortem analysis. Blood samples will be collected prior to and following injury via the right femoral access site. Measurement of CRP will be conducted in a similar manner as described in Specific Aim 1a. Temperature measurements will be obtained using an expanding basket catheter that allows contact of thermistors with the arterial walls (Figure 1). This was demonstrated in the section on preliminary data.

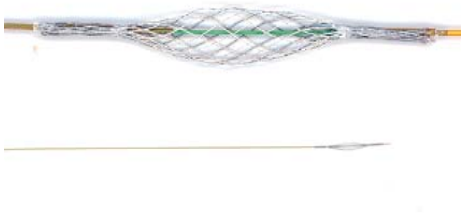

Figure 1. (Top) Basket catheter tip with expanding mesh that brings the thermistors in contact with the arterial wall. (Bottom) full catheter body (4F) that can be advanced from the femoral vein to map the temperature of the entire aorta.

Aim 2b. Immunohistochemistry methods will be performed using the aortas from rabbits subjected to temperature measurements in Specific Aim 2a and 3a. Markers used for immunohistochemistry include TF, PAI-1, CRP and CD40/CD40L. Temperature and thrombus will be correlated based on the post-mortem analysis and localization. Arterial wall cholesterol will be measured and correlated to the immunohistochemical markers and temperature.

Aim 2c. Antibodies to inflammatory molecules will be used in this setting to determine if temperature response can be normalized.

Aim 3a will determine heat released during thrombosis. Experiments have been performed in the past, attempting to measure this energy release using a water bath. However, the large mass and specific heat of the water bath imparts a damping effect on the temperature rise of the blood sample. This temperature rise should otherwise be observable in a sample isolated from its surroundings. Because of difficulty in detecting temperature change *in vivo* or in areas with large thermal sinks, it is necessary to determine the temperature changes in a thermally isolated setting. In order to accomplish this, blood samples will be placed in a series of test tubes held in an insulating polystyrene holder. The insulated holder will in turn be placed in an insulated enclosure, heated to the ambient temperature of the test tubes to minimize the temperature difference between the air and the small portion of the tubes exposed to the air. Additionally, this heated space will be used to bring all of the test tubes to a uniform temperature just prior to the start of the experiment (Figure 2).

Blood is drawn from rabbits and placed in several test tubes. These are then placed in a polystyrene block, which is drilled to facilitate a tight fit for the tubes, so as to avoid the circulation of air around the outside surface of the tubes. The tubes extend very little above the top surface of the polystyrene block, only as necessary to permit removal. The top surface of the tubes is also covered with an insulating blanket. This minimizes the potential for convective heat transfer from the air to the blood or vise versa. The primary objective is to trap any heat released by the reaction associated with clotting to the volume of the blood and the test tubes. Each tube is provided with two thermocouples for redundancy, with one located in the upper part of the tube and one in the lower part. The thermocouples in turn are read by a data acquisition system. Additionally, two thermocouples are placed in the experimental chamber to record the average chamber air temperature throughout the experiment.

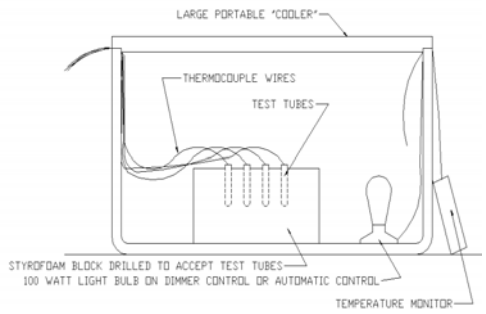

Figure 2. Clotting Calorimeter Experiment. Blood samples will be taken and placed in a series of test tubes held in an insulating polystyrene holder. Clotting will be induced by the addition of Thrombin. Temperature measurements as a function of time can be recorded by a data acquisition system throughout the experiment.

Once the blood has been added to the test tubes, temperature measurements from the thermocouples through data acquisition system can be observed and recorded. Certain time is required during this transient period to allow the samples to come to thermal equilibrium. Once changes in temperature with respect to time have subsided, the clotting can be induced by addition of thrombin and formal recording of temperature with respect to time can begin. The readings on all thermocouples in all tubes are recorded at intervals not greater than 30 seconds. Additionally, temperature of the air in the chamber is recorded at the same interval. As the chemical reactions associated with the clotting take place, the heat given off raises the temperature of the test tube and the blood with a negligible amount of heat lost to the surroundings, due to the insulating properties of the polystyrene block and the blanket cover.

Temperature measurements are taken until the temperature rise resulting from the heat released from the clotting reaction appears to stop. This is evidenced by a stabilization of the temperature, wherein the temperature appears to no longer rise as a function of time. At this apparent stabilization point, the experiment is continued and measurements are recorded until the overall time past the stabilization point is equal to the time of stabilization, as measured from the point of the introduction of the thrombin at the start of the experiment. The purpose of recording the extended post-stabilization data is for analysis of heat loss rates from the tubes in the experimental enclosure. Each year, blood from normal (n=10); atherosclerotic (n=20) and thrombus triggered rabbits (n=20) will be used and compared to determine any differences that may be altered by varying systemic conditions.

Aim 3b will involve direct numerical temperature profiles for arteries in which injuries or clotting have taken place. For computing the temperature in the artery wall, thermal conduction will be assumed, in cylindrical coordinates, with a convective surface on the interior and either a convective surface or a semi-

infinite solid boundary condition on the exterior. Due to the potential irregularities in the region on the injury, a numerical solution will be developed. The full three-dimensional transient heat conduction equation in cyclindrical coordinates, with constant properties is

$$\frac{1}{r}\frac{\partial}{\partial r}\left(r\frac{\partial T}{\partial r}\right)+\frac{1}{r^2}\frac{\partial}{\partial \theta}\left(r\frac{\partial T}{\partial \theta}\right)+\frac{\partial^2 T}{\partial z^2}+g=\frac{1}{\alpha}\frac{\partial T}{\partial t}$$

where r is the distance from the centerline of the artery, θ is the circumferential coordinate, z is the axial coordinate, t is time, and T is the temperature as a function of r, θ, z and, t. Additionally, α is the thermal diffusivity and g is the volume energy generation rate as a function of r, θ, z and, t.

Given the relatively small size of arteries, on the order of centimeters, and the accompanying long time associated with the duration of the anticipated heat generation, on the order of tens of minutes, it should be reasonable to consider the heat conduction in the artery to be steady-state. This can be verified by considering the dimensionless time for a transient of this duration, assuming a thermal diffusivity of approximately 10^{-7} m^2/s. Using these assumptions gives

$$t^* = \frac{\alpha t}{L^2} = \frac{(10^{-7})(1200)}{(.01)^2} = 1.2$$

With a dimensionless time greater than 1, the conduction transient following the injury is nearly complete. Therefore, a steady state analysis is not unreasonable. A geometric simplification can be employed as well. A two dimensional analysis could be used when variations are expected to be minimal in one of the three dimensions in the cylindrical coordinate system, depending upon the location and size of the injured area of the artery. If a long injury or clot along one side of an artery is to be examined, variation of temperature in the axial direction could be ignored and variations in the radial and circumferential directions could be calculated. An illustration for a sample grid for this type of situation is shown in Figure 3.

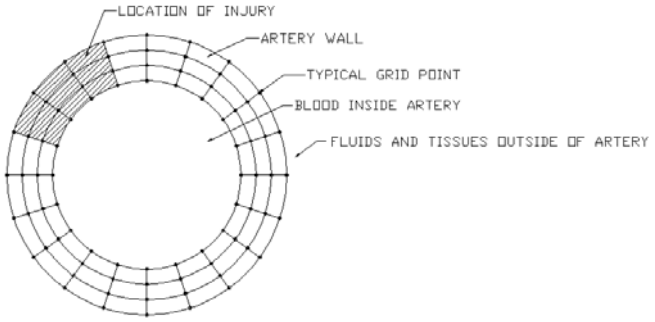

Figure 3. Two dimensional numerical grid for calculation of temperatures in the artery for a circumferentially dependent orientation of an injury site. This is a two dimensional problem which can be computed much more rapidly than a three-dimensional case, and is best suited for small local injuries.

In this case, the differential equation would reduce to

$$\frac{1}{r}\frac{\partial}{\partial r}\left(r\frac{\partial T}{\partial r}\right)+\frac{1}{r^2}\frac{\partial}{\partial \theta}\left(r\frac{\partial T}{\partial \theta}\right)+g=0$$

with boundary conditions on the inside and outside surfaces, respectively, of

$$k\left.\frac{\partial T}{\partial r}\right|_{r=r_i} = h_i\left(T(r=r_i) - T_{blood}\right)$$

$$k\left.\frac{\partial T}{\partial r}\right|_{r=r_o} = h_o\left(T_{fluids} - T(r=r_o)\right)$$

The internal energy generation term would only apply in the affected area modeling the injury. Elsewhere it would be zero. Similarly, if an injury is assumed to completely surround the artery in one location, variation in the circumferential direction could be ignored and the radial and axial dimensions alone could be considered. This situation is depicted in Figure 4, where a two dimensional finite difference grid is shown in the axial and radial directions. In this case, the applicable differential equation is

$$\frac{1}{r}\frac{\partial}{\partial r}\left(r\frac{\partial T}{\partial r}\right) + \frac{\partial^2 T}{\partial z^2} + g = 0$$

with boundary conditions on the inside and outside surfaces, respectively, of

$$k\left.\frac{\partial T}{\partial r}\right|_{r=r_i} = h_i\left(T(r=r_i) - T_{blood}\right)$$

$$k\left.\frac{\partial T}{\partial r}\right|_{r=r_o} = h_o\left(T_{fluids} - T(r=r_o)\right)$$

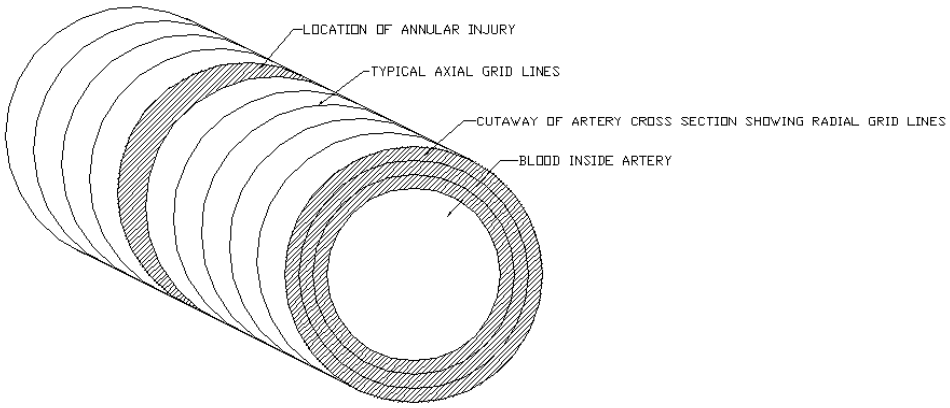

Figure 4. Two dimensional numerical grid for calcula- calculation of temperatures in the artery for an axially dependent orientation of an injury site. This is a two dimensional problem which can be computed much more rapidly than a three-dimensional case and is best suited for cases where the injury exists over the entire circumference of the artery.

The internal energy generation term would only apply in the affected area modeling the injury. Elsewhere it would be zero. Both of these differential equations could be solved for various sizes and configurations of injuries, so as to be correlated with the experimental measurements and applied using the inverse methods in Specific Aim 3c. These equations are anticipated to be solved using a custom made finite difference method, as opposed to using a commercial software package because of the repetitions to be used by the inverse methods.

Aim 3c will involve the analysis of experimentally measured data from Specific Aim 2. Temperature measurements can be taken using a thermal catheter *in vivo*, measuring the temperature response to injury or clotting. Temperature measurements taken by the thermal catheter can be fitted using inverse heat transfer analysis (47). The essence of the procedure is to compute values of temperature rise, as functions of position and time, in the artery in response to a unit volumetric energy generation rate within a certain number of finite control volumes within the grid. Assuming that one of the two dimensional steady state

grid systems mentioned in Aim 3b is to be used, the computation will depend only on position in two dimensions with no dependence on time. This can be expressed as a function which is typically designated as $\varphi_{i,j}(r,\theta)$ or $\varphi_{i,j}(r,z)$ depending on whether the problem is being considered in the z or the θ direction. In either case, the i and j subscripts designate the location of the internal energy generation, in terms of which finite control volume contains the internal energy generation. Using a numerical grid solution, the r, θ and z dimensions can be thought of as indices as well. Therefore, for each point on the grid, a temperature rise given by $\varphi_{i,j}(r,\theta)$ or $\varphi_{i,j}(r,z)$ will be calculated. There will be as many values of the unit temperature function as there are finite control volumes in the grid for each point on the grid. Of course, many of these are redundant and will not need to be calculated, but there are potentially thousands of these function values.

Using the principle of superposition, the actual temperature rise at a given point in the grid will be the sum of the contributions from each of the finite control volumes. With the unit temperature rise functions $\varphi_{i,j}(r,\theta)$ or $\varphi_{i,j}(r,z)$ calculated and tabulated, this temperature rise will be the sum of each of the individual functions multiplied by the magnitude of the internal energy generation in the corresponding finite control volume. This is

$$T(r,\theta)=\sum_{\substack{i=1\\j=1}}^{\substack{i=m\\j=n}} g_{i,j}\phi_{i,j}(r,\phi) \qquad or \qquad T(r,z)=\sum_{\substack{i=1\\j=1}}^{\substack{i=m\\j=n}} g_{i,j}\phi_{i,j}(r,z)$$

where $g_{i,j}$ is the magnitude of the internal energy generation in the finite control volume with indices i and j and m and n are the number of nodes in the r and θ or the r and z directions, respectively. Given a collection of temperature measurements with respect to position, the location and magnitude of the heating in the artery due to injury or clotting can be computed. This method then gives a quantitative measure of the location and extent of injury or disease in the artery.

Aim 4a. Rabbit thrombi *in vitro* and *in vivo* will be ablated by UV excimer laser (308 nm excimer laser, Spectranetics CVS-300^{TM}, Spectranetics, Colorado Springs, CO) with 0.7, 0.9, 1.7 and 2.0 mm diameter optical fibers. Saline is flowed through the central hole by a syringe pump. Within the laser ablation the fiber is pushed through the thrombus by a hand-control micrometer and the speed depends on the laser power. As a control, some tests are done with only fiber without laser to test the mechanical effect on thrombus. The buffer with the ablated debris is collected in a beaker. After treatment the buffer is centrifuged to separate the debris. The debris is dried and weighted. The remaining thrombus in the tube is dried at 70^{o}C over night (48, 49). Meanwhile, some tubes with thrombus are dried without treatment and weighed to calculate the ratio of wet/dry weight of thrombus. The lost thrombus weight is calculated from this ratio and the remaining thrombus dry weight. Particle size measurement is done by a modified Coulter counter and laser scattering method. The Coulter counter's output pulse signal is converted to digital signal by the A-D converter in the controller of a multi-channel analyzer and recorded as a computer data file. The pulse high (proportion to particle volume) distribution is calculated with a home-written software.

Aim 4b. CRP, PAI-1 and TF in the serum of rabbits (lased and non-lased) will be measured with ELISA and the protein contents will be correlated to the thrombus formation/ablation and platelet activity.

In the whole project, rabbits will be used as the multi-purpose. Endothelium and smooth muscle cells from hearts and arteries of the 3 rabbit groups will be primary cultured for the reference observation and histology will be made by the standard method.

Data Analysis: The temperature rise as a function of time is plotted at the conclusion of the experiment, including measurements taken beyond the stabilization time. Using the values available for the mass and specific heat of the glass test tube and the blood, the amount of heat released can be determined by the product of these two quantities and the temperature change. Using the measurements from the post-stabilization period, the rate of heat lost from the test tubes as a function of the temperature difference between the tubes and the experimental chamber can be computed, namely an effective convection coefficient. From this effective convection coefficient, the quantity of heat loss during the experiment is computed and is added to the heat release computed from the temperature rise in the test tubes in order to compute the total amount of heat released in the clotting reaction. The heat released during the clotting process on a per-gram basis will then be known, which can be used in other analyses where temperature is measured in connection with clotting and injury. This in turn, using inverse heat transfer techniques, allows

an analysis of the magnitude of clotting and injury having taken place when only temperature measurements are available.

Data comparing the three groups will be compared using a Student's t-test. Also, multivariate analysis will be made comparing the serum level of CRP, IL-6 and other inflammation markers relative to the temperature elevation achieved. Each group of rabbits will consist of 10 to 20 animals. These are powered to be able to distinguish significant differences based on the probability of less than 0.05.

Expected Findings/Potential Problems: It is expected that we will see a significant temperature rise, on the order of several degrees Celsius, as heat is released from the reactions associated with clotting. The stabilization point is expected to occur in the neighborhood of 20 to 30 minutes after the addition of the thrombin. The rate of heat loss from the samples to the surroundings of the experimental enclosure is expected to be negligible or nearly so. But, it is also possible that the temperature rise may not be measurable by the means of detection employed. Because thrombus continues to contract for many hours, temperature monitoring many need to be followed for up to 24 hours. Thus, the point of stabilization may also be somewhat different from that anticipated, which would require the experiment to be repeated with a different sampling frequency.

It is expected that a temperature rise can be calculated throughout the tissue of the artery in response to heating due to an injury in a particular location. It is also expected that it will be possible to correlate these numerical results with empirical measurements taken *in vivo* as part of Specific Aim 2. A potential problem is in attempting to estimate the size and shape of the injury used in the empirical measurements in order to make the correlation with the numerical model. Physical examination of the injury site for the artery used may be necessary in order to better estimate the size and location of the injury. Additionally, the injury may resemble neither the size nor shape. In this case, a three dimensional model may be required, which would be considerably more computationally expensive, requiring a considerably more complicated program as well. This would reduce the potential output in terms of results that could be generated for the thermal aspects of the injuries in the artery wall.

For the *in vivo* measurements, the small temperature rises anticipated, which are only expected to be one order of magnitude above the limit of detection of the thermal catheter at best, dictates that measurement errors will be large in comparison to the temperature rise. This brings about a significant challenge in the application of inverse methods. Similarly, the difficulty associated with determining the location of the catheter, both axially and circumferentially, during the *in vivo* measurement of temperature adds to the challenge imposed on the inverse thermal analysis.

Advantages of the Method: (1) Nearly all thermal energy released from the reaction is accounted for by observing temperature rise. (2) Heat lost to the surroundings can be accounted for by watching temperature decay with no accompanying heat generation. (3) Thermal energy released can be examined in isolation without the interfering influenced of an *in vivo* experiment.

Correspondence to:
Ma Hongbao
Michigan State University
East Lansing, MI 48824, USA
mahongbao2000@yahoo.com

References

1. Abela GS, Picon PD, Friedl SE, Gebara OC, Federman M, Tofler GH, Muller JE. Triggering of plaque disruption and arterial thrombosis in an atherosclerotic rabbit model. Circulation 1995;91:776-784.
2. Ma H, Huang R, Abela GS. Excimer laser irradiation alters platelet aggregation based on total energy. Lasers in Medicine and Surgery 2004;16 (Supplement):6.
3. Buffon A, Liuzzo G, Biasucci LM, Pasqualetti P, Ramazzotti V, Rebuzzi AG, Crea F, Maseri A. Preprocedural serum levels of C-reactive protein predict early complications and late restenosis after coronary angioplasty. J Am Coll Cardiol 1999;34:1512-1521.
4. Fujimori Y, Morio H, Terasawa K, Shiga T, Hatano M, Osegawa M, Uchida Y, Morita T. Multiple plaque ruptures in patients with acute myocardial Infarction: an angioscopic evidence of systemic cause of plaque instability. J Am Coll Card 2002;37:307A.

5. Rioufol G, Finet G, Ginon I, Andre-Fouet X, Rossi R, Vialle E, Desjoyaux E, Convert G, Huret JF, Tabib A. Multiple atherosclerotic plaque rupture in acute coronary syndrome: a three-vessel intravascular ultrasound study. Circulation 2002;106:804-808.
6. Chang MK, Binder CJ, Torzewski M, Witztum JL. C-reactive protein binds to both oxidized LDL and apoptotic cells through recognition of a common ligand: Phosphorylcholine of oxidized phospholipids. Proc Natl Acad Sci USA 2002;99(20):13043-13048.
7. Aronow WS, Ahn C. Prevalence of coexistence of coronary artery disease, peripheral arterial disease, and atherothrombotic brain infarction in men and women > or = 62 years of age. Am J Cardiol 1994;74(1):64-65.
8. Salonen JT, Salonen R. Ultrasonographically assessed carotid morphology and the risk of coronary heart disease. Arterioscler Thromb 1991;5:1245-1249.
9. Ridker PM, Stampfer MJ, Rifai N. Novel risk factors for systemic atherosclerosis: a comparison of C-reactive protein, fibrinogen, homocyteine, lipoprotein (a), and standard cholesterol screening as predictors of peripheral vascular disease. JAMA 2001;285:2481-2485.
10. Torzewski M, Rist C, Mortensen RF, Zwaka TP, Bienek M, Waltenberger J, Koenig W, Schmitz G, Hombach V, Torzewski J. C-reactive protein in the arterial intima: role of C-reactive protein receptor-dependent monocyte recruitment in atherogenesis. Arterioscler Thromb Vasc Biol 2000;20(9):2094-2099.
11. Cermak J, Key NS, Bach RR, Balla J, Jacob HS, Vercellotti GM. C-reactive protein induces human peripheral blood monocytes to synthesize tissue factor. Blood 1993;82(2):513-520.
12. Kohler P, Grant PJ. Plasminogen-activator inhibitor type 1 and coronary artery disease. N Engl J Med 2000;342:1792–1801.
13. Vassalli JD, Sappino AP, Belin D. The plasminogen activator/plasmin system. J Clin Invest 1991;88;1067–1072.
14. van Meijer M, Pannekoek H. Structure of plasminogen activator inhibitor 1 (PAI-1) and its function in fibrinolysis: an update. Fibrinolysis 1995;9:263–276.
15. Böhm T, Geiger M, Binder BR. Isolation and characterization of tissue-type plasminogen activator–binding proteoglycans from human umbilical vein endothelial cells. Arterioscler Thromb Vasc Biol 1996;16:665-672.
16. Aronson D, Bartha P, Zinder O, Kerner A, Shitman E, Markiewicz W, Brook GJ, Levy Y. Association between fasting glucose and C-reactive protein in middle-aged subjects. Diabet Med 2004;21(1):39-44.
17. Vague J, Alessi MC. PAI-1 and atherothrombosis. Thromb Hemost 1993;70:138–153.
18. Lijnen HR, Collen D. Mechanism of physiological fibrinolysis. Baillieres Clin Hematol 1995;8:277–290.
19. Vaughan DE, Declerck PJ, Van Houtte E, De Mol M, Collen D. Reactivated recombinant plasminogen activator inhibitor-1 (rPAI-1) effectively prevents thrombolysis *in vivo*. Thromb Haemost 1992;68(1):60-63.
20. Levi M, Biemond BJ, van Zonneveld AJ, ten Cate JW, Pannekoek H. Inhibition of plasminogen activator inhibitor-1 activity results in promotion of endogenous thrombolysis and inhibition of thrombus extension in models of experimental thrombosis. Circulation 1992;85(1):305-312.
21. Friederich PW, Levi M, Biemond BJ, Charlton P, Templeton D, van Zonneveld AJ, Bevan P, Pannekoek H, ten Cate JW. Novel low-molecular-weight inhibitor of PAI-1 (XR5118) promotes endogenous fibrinolysis and reduces postthrombolysis thrombus growth in rabbits. Circulation 1997;96(3):916-921.
22. Eren M, Painter CA, Atkinson JB, Declerck PJ, Vaughan DE. Age-dependent spontaneous coronary arterial thrombosis in transgenic mice that express a stable form of human plasminogen activator inhibitor-1. Circulation 2002;106:491–496.
23. van Kooten C, Banchereau J. CD40-CD40 ligand. J Leukoc Biol 2000;67:2–17.
24. Mach F, Schonbeck U, Sukhova GK, Bourcier T, Bonnefoy JY, Pober JS, Libby P. Functional CD40 ligand is expressed on human vascular endothelial cells, smooth muscle cells, and macrophages: implications for CD40-CD40 ligand signaling in atherosclerosis. Proc Natl Acad Sci USA 1997;94:1931–1936.
25. Henn V, Slupsky JR, Grafe M, Anagnostopoulos I, Forster R, Muller-Berghaus G, Kroczek RA. CD40 ligand on activated platelets triggers an inflammatory reaction of endothelial cells. Nature 1998;391:591–594.

26. Slupsky JR, Kalbas M, Willuweit A, Henn V, Kroczek RA, Muller-Berghaus G. Activated platelets induce tissue factor expression on human umbilical vein endothelial cells by ligation of CD40. Thromb Haemost 1998;80:1008–1014.
27. Lindmark E, Tenno T, Siegbahn A. Role of platelet P-selectin and CD40 ligand in the induction of monocytic tissue factor expression. Arterioscler Thromb Vasc Biol 2000;20(1):2322-2328.
28. Aukrust P, Muller F, Ueland T, Berget T, Aaser E, Brunsvig A, Solum NO, Forfang K, Froland SS, Gullestad L. Enhanced levels of soluble and membrane-bound CD40 ligand in patients with unstable angina. Possible reflection of T lymphocyte and platelet involvement in the pathogenesis of acute coronary syndromes. Circulation 1999;100(6):614-620.
29. Misumi K, Ogawa H, Yasue H, Soejima H, Suefuji H, Nishiyama K, Takazoe K, Kugiyama K, Tsuji I, Kumeda K, Nakamura S. Comparison of plasma tissue factor levels in unstable and stable angina pectoris. Am J Cardiol 1998;81:22–26.
30. Annex BH, Denning SM, Channon KM, Sketch MH Jr, Stack RS, Morrissey JH, Peters KG. Differential expression of tissue factor protein in directional atherectomy specimens from patients with stable and unstable coronary syndromes. Circulation 1995;91:619–622.
31. Tracy R. Atherosclerosis, thrombosis and inflammation: a question of linkage. Fibrinolysis Proteolysis. 1997;11(supplement 1):137–142.
32. Nakagomi A, Freedman SB, Geczy CL. Interferon-gamma and lipopolysaccharide potentiate monocyte tissue factor induction by C-reactive protein: relationship with age, sex, and hormone replacement treatment. Circulation 2000;101(15):1785-1791.
33. Casscells W, Hathorn B, David M, Krabach T, Vaughn WK, McAllister HA, Bearman G, Willerson JT. Thermal detection of cellular infiltrates in living atherosclerotic plaques: possible implic thermal detection of cellular infiltrates in living atherosclerotic plaques: possible implications for plaque rupture and thrombosis. Lancet 1996 25;347(9013):1422-1423.
34. Stefanadis C, Diamantopoulos L, Vlachopoulos C, Tsiamis E, Dernellis J, Toutouzas K, Stefanadi E, Toutouzas P. Thermal heterogeneity within human atherosclerotic coronary arteries detected *in vivo*: A new method of detection by application of a special thermography catheter. Circulation 1999;99(15):1965-1971.
35. Anderson, Valvanao J. Small artery heat transfer model for self-heated thermistor measurements of perfusion on the kidney cortex. Journal of Biomechanical Engineering (ASME) 1994;116(1):71-78.
36. Roemer R. Conditions for equivalency of countercurrent vessel heat transfer formulations. Journal of Biomechanical Engineering (ASME) 1999;121(5):514-520.
37. Zhu L, Weinbaum S. Model for heat transfer from embedded blood vessels in two-dimensional tissue preparations. Journal of Biomechanical Engineering (ASME) 1995;117:64-73.
38. Klemick SG, Jog MA, Ayyaswamy PS. Numerical evaluation of heat clearance properties of a radiatively heated biological tissue by adaptive grid scheme. Numerical Heat Transfer (Part A): Applications 1997;31(5):451-467.
39. Chan C. Boundary element method analysis for the bioheat transfer equation. Journal of Biomechanical Engineering (ASME) 1992;114(3):358-365.
40. Ma H, Huang R, Hage-Korban E, Maheshwari A, Qiao X, Dickinson MG, Abela GS. Arterial Wall Tissue Content of Cholesterol Directly Correlates with the Extent of Arterial Thrombosis After an Acute Vascular Event. FASEB Experimental Biology 2003;8(LB38).
41. Ma H, Claycombe K, Huang R, Abela GS. C-reactive protein rise is associated with the development of acute events in a model of plaque rupture and thrombosis. FASEB Journal 2004;18(8):C193-194.
42. Ma H, Huang R, Prieto AR, Abela GS. Pravastatin preserves vasomotor response in atherosclerotic arteries after balloon angioplasty. FASEB Experimental Biology 2002;48(LB244).
43. Hage-Korban EE, Ma H, Prieto AR, Qiao X, Akhrass F, Huang R, Abela GS. Beta-carotene preserves endothelium dependent relaxation in an atherosclerotic model of plaque disruption and thrombosis. Am Coll Phys 1999.
44. Abela GS, Huang R, Ma H, Prieto AR, Lei M, Schmaier AH, Schwartz KA, Davis JM. Laser-light scattering, a new method for continuous monitoring of platelet activation in circulating fluid. J Lab Clin Med 2003;141(1):50-57.
45. Prieto AR, Ma H, Huang R, Khan G, Schwartz KA, Hage-Korban EE, Schmaier AH, Hasan AAK, Abela GS. Thrombostatin, a bradykinin metabolite, reduces platelet activation in a model of arterial wall injury. Cardiovascular Research 2002;53(4):984-992.

46. Ma H, Huang R, Abela GS. Heat shock protein 70 expression is reduced in rat myocardium following transmyocardial laser revascularization. Journal of Investigative Medicine 2004;52:36.
47. Beck J, Blackwell B, St Clair C. Inverse Heat Conduction - Ill Posed Problems, Wiley, New York, 1985.
48. Papaioannou T, Levinsman J, Sorocoumov O, Taylor K, Pitzer Shane, Grundfest WS. Particulate debris analysis during excimer laser thrombolysis: An *in vitro* study. Lasers in Surgery: SPIE 2002;4609:404-411.
49. Papaioannou T, Sorocoumov O, Taylor K, Grundfest WS. Excimer laser assisted thrombolysis: The effect of fluence, repetition rate and catheter size. Lasers in Medicine: Proc SPIE 2002;4609:413-418.